Application of Cohesive Elements for the Simulation of Crack Extension

Wolfgang Brocks [1,a] and Ingo Scheider [2,b]

[1] Institute for Materials Science, Christian-Albrecht University, Kaiserstr 2, D-24143 Kiel, Germany

[2] Helmholtz-Zentrum Geesthacht, Institute of Materials Research, Materials Mechanics, Max Planck Str, D-21502 Geesthacht, Germany

[a] wbrocks@kabelmail.de, [b] ingo.scheider@hzg.de

Keywords: numerical simulation of crack extension, cohesive elements, traction-separation law

Abstract. The concept of a cohesive interface at the boundary of adjacent continuum elements that allows for material separation is a useful, versatile and well-established tool for many kinds of fracture mechanisms. The cohesive zone is a phenomenological model but based upon a sound physical background. Cohesive models can be applied to problems with or without initial cracks, i.e. classical fracture mechanics as well as debonding problems. As they represent a local approach, they are less sensitive to any geometry dependence of their parameters.

Introduction

As R-curves based on classical parameters of fracture mechanics like J or CTOD suffer from geometry dependence and have limited predictive capabilities, new concepts like continuum damage mechanics and cohesive models have emerged and find increasing interest, all necessitating computational tools. Cohesive elements have in particular proven their ability in modelling crack extension in thin-walled panels and shells, and the respective model parameters provide physically meaningful measures of the materials fracture toughness and tearing resistance. The general concept is attributed to Barenblatt [1, 2] who introduced a cohesive zone in the ligament of the crack, where material degradation occurs, in order to avoid the unphysical singularity in linear elastic fracture mechanics, Fig. 1a.

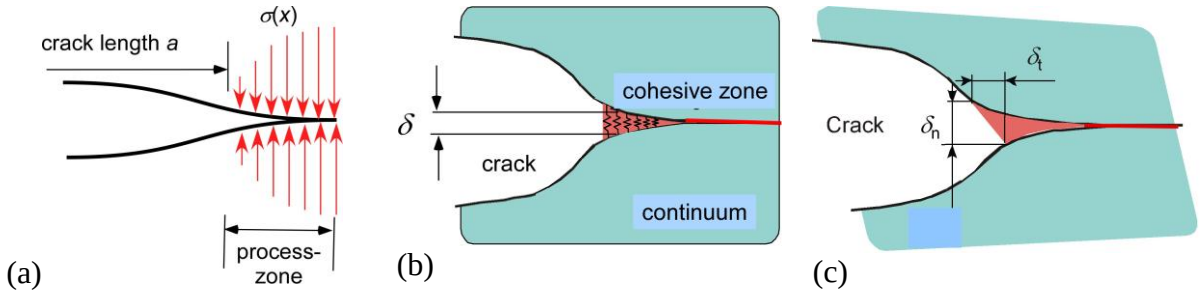

Fig.1. Concept of a cohesive zone ahead of a crack tip: (a) Barenblatt's model, (b) continuum and cohesive zone; (c) mixed-mode separation.

As the actual distribution of stresses, $\sigma(x)$, is unknown and is not measurable, either, the idea has been modified by introducing a *cohesive law*, $\sigma(\delta)$, instead, with *cohesive stresses* or *tractions* in dependence on the local *separation*, $\delta = \Box u \Box = u^{+} - u^{-}$, which denotes the discontinuity in the

displacement field in the cohesive zone, Fig 1b, c. The model became particularly interesting for practical applications when numerical methods for solving nonlinear problems like the finite element method (FEM), became available.

The Cohesive Model – General Description

Traction-Separation Law. The concept of a *traction-separation law* (TSL) was first used by Hillerborg et al. [3] for analysing crack formation and crack growth in concrete. It is the base for all modern realisations of the cohesive model in the framework of FEM. Cohesive stresses or *tractions* and separation are vectors, $\boldsymbol{\sigma} = \{\sigma_n, \sigma_t, \sigma_s\}$ and $\boldsymbol{\delta} = \{\delta_n, \delta_t, \delta_s\}$, in general, having one normal component, σ_n and δ_n (corresponding to mode I), respectively, and two tangential components, σ_t, σ_s and δ_t, δ_s, respectively, For isotropic materials the two tangential separation laws are identical, leaving two functions, $\sigma_n(\delta_n,\delta_t)$ and $\sigma_t(\delta_n,\delta_t)$, to be determined, Fig 1c.

Tractions become zero if critical separations δ_n^c or δ_t^c are reached. The maximum stresses, σ_n^c and σ_t^c, called *cohesive strengths* are introduced as model parameters. An integration of the traction-separation curve yields the mechanical work per crack increment which has been dissipated during the course of damage until final separation,

$$\Gamma_n^c = \int_0^{\delta_n^c} \sigma_n(\delta_n)\big|_{\delta_t=0}\,\mathrm{d}\delta_n \quad \text{and} \quad \Gamma_t^c = \int_0^{\delta_t^c} \sigma_t(\delta_t)\big|_{\delta_n=0}\,\mathrm{d}\delta_t\,, \tag{1}$$

for normal and shear separation, respectively. These *separation energies* represent critical *energy release rates* in Griffith' sense [4] and can be used as model parameters alternatively to the critical separations. For quasi-static ductile crack extension, Γ_n^c equals the *J*-integral of Rice at initiation under mode I assuming deformation theory, and for real materials governed by incremental theory of plasticity,

$$\Gamma_n^c \le J_i \tag{2}$$

holds. Different from constitutive equations of continuum mechanics, which represent relations between stresses and strains resulting in an energy per volume,

$$w = \int \sigma_{ij}\dot{\varepsilon}_{ij}\,dt\,, \tag{3}$$

cohesive laws are relations between stresses and displacements and the respective integrals of eq. (1) result in energies per area. This constitutes an essential difference between damage models and cohesive models with respect to mesh sensitivity.

The specific shapes of cohesive laws depend on the respective separation mechanisms. There is hence a variety of approaches in the literature, see e.g. overviews in [5, 6] and Fig. 2. Their adequacy to describe crack extension in a structure can be evaluated by comparisons between macroscopic experimental data and numerical simulation results. For certain damage mechanisms one may also conclude from micromechanical simulations to the cohesive law, e.g. [7, 8], and hence assign some micromechanical interpretation to the model parameters cohesive strength and separation energy [4]. Initially, all models were established for cracks of pure mode I under monotonic loading. Improvements and enhancements have been developed for mixed-mode loading, unloading and reloading, time dependence, cyclic loading and dependencies on various state variables like triaxiality, strain rate etc.

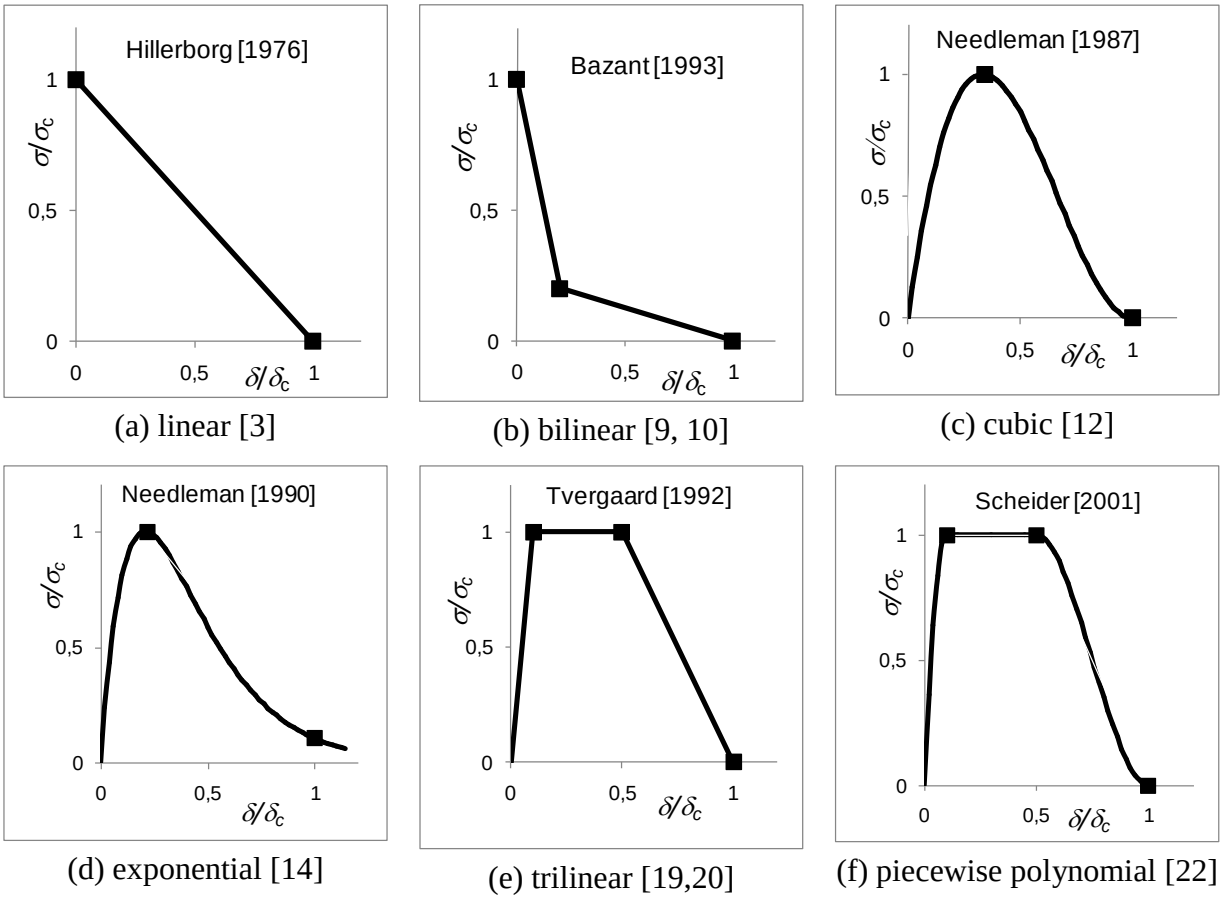

(a) linear [3] (b) bilinear [9, 10] (c) cubic [12]

(d) exponential [14] (e) trilinear [19,20] (f) piecewise polynomial [22]

Fig. 2. Various traction-separation laws proposed and applied in the literature

Hillerborg et al. [3] analysed crack formation and crack growth in concrete with their *linear* law, Fig. 2a, which is generally applicable to brittle mineral materials. A *bilinear* modification by Bažant [9, 10] introducing two additional shape parameters, namely δ_1, σ_1 at the inflexion point, Fig. 2b, yields a more realistic description of fracture in concrete [11].

Needleman [12] introduced a *cubic* function, Fig. 2c, for ductile materials in mode I,

$$\sigma = \sigma_c \frac{27}{4}\frac{\delta}{\delta_c}\left(1-\frac{\delta}{\delta_c}\right)^2 \quad , \qquad \Gamma_c = \tfrac{9}{16}\sigma_c\delta_c \, , \tag{4}$$

which Tvergaard [14] applied in mode II for simulating the debonding of fibres in a fibre reinforced metal. The *exponential* TSL, Fig. 2d, by Needleman [14]

$$\sigma = \sigma_c \frac{16}{9}e^2\frac{\delta}{\delta_c}\exp\left(-\frac{16}{9}e\frac{\delta}{\delta_c}\right) , \qquad \Gamma_c = \tfrac{9}{16}\sigma_c\delta_c \ , \tag{5}$$

where $e=\exp(1)$ has been derived from a potential of atomic binding forces for metals and bimetallic interfaces [15]. A characteristic of this function is that cohesive stresses do not vanish for $\delta=\delta_c$ but take the value of $\sigma(\delta_c)=0.105\sigma_c$. The separation energy, Γ_c, is the same as for the cubic function, eq. (4). It has been applied to dynamic fracture in brittle solids [16, 17] as well as for ductile materials [7, 18].

Tvergaard and Hutchinson [19, 20] proposed a *tri-linear* separation law with a partly constant stress in the range of $\delta_1 \le \delta \le \delta_2$, Fig. 2e,

$$\sigma = \sigma_c \begin{Bmatrix} \dfrac{\delta}{\delta_1} & \delta \le \delta_1 \\ 1 & \delta_1 \le \delta \le \delta_2 \\ \dfrac{\delta_c - \delta}{\delta_c - \delta_2} & \delta_2 \le \delta \le \delta_c \end{Bmatrix}, \qquad \Gamma_c = \tfrac{1}{2}\sigma_c \delta_c \left(1 - \frac{\delta_1}{\delta_c} + \frac{\delta_2}{\delta_c}\right), \qquad (6)$$

for ductile crack extension in modes I and II. The two additional *shape parameters*, δ_1 and δ_2, increase its flexibility to characterise various separation processes. In Fig. 2e $\delta_1 = 0.1\delta_c$ and $\delta_2 = 0.5\delta_c$ have been chosen. As special cases, Hillerborg's model follows for $\delta_2 = \delta_1 \to 0$ and the constant stress model [21] for $\delta_1 \to 0$, $\delta_2 \to \delta_c$. Scheider's *piecewise polynomial* [22, 23], Fig. 2f,

$$\sigma = \sigma_c \begin{Bmatrix} 2\left(\dfrac{\delta}{\delta_1}\right) - \left(\dfrac{\delta}{\delta_1}\right)^2 & \delta \le \delta_1 \\ 1 & \delta_1 \le \delta \le \delta_2 \\ 2\left(\dfrac{\delta - \delta_2}{\delta_c - \delta_2}\right)^3 - 3\left(\dfrac{\delta - \delta_2}{\delta_c - \delta_2}\right)^2 + 1 & \delta_2 \le \delta \le \delta_c \end{Bmatrix}, \quad \Gamma_c = \tfrac{1}{2}\sigma_c \delta_c \left(1 - \frac{2}{3}\frac{\delta_1}{\delta_c} + \frac{\delta_2}{\delta_c}\right) \qquad (7)$$

resembles the tri-linear function of Tvergaard and Hutchinson but is continuously differentiable in the transition points. For $\delta_1 = \delta_2 = 0.33\delta_c$ it comes close to the cubic function of Needleman, Fig. 2c, eq. (4). Scheider & Brocks [24] applied eq. (7) to a *mixed-mode* problem with crack bifurcation, namely the simulation of cup-cone fracture in a round tensile bar.

The shape parameter δ_2 in eqs. (6) and (7) is specific for a given separation process and hence part of the identification process of cohesive parameters, in general, whereas δ_1, is predominantly of numerical importance. The cohesive elements are supposed to describe the degradation of the material but no elastic or inelastic deformations, which is the business of the continuum elements. The initial *compliance* of the $\sigma(\delta)$-Kurve, $\delta_1/\sigma_c = 1/E_{coh}$, though numerically inevitable, should hence be as small as possible [25], $E/(E_{coh}\Delta) \gg 1$, E being Young's modulus and Δ the *element size* in the ligament, that is

$$\delta_1/\Delta \ll 1. \qquad (8)$$

A high initial compliance of the separation law may result in numerical artefacts during the simulations. It is some drawback of the separation laws of Needleman, Fig. 2c,d, eqs. (4), (5), that the initial compliances cannot be chosen independently of the cohesive parameters, σ_c und δ_c,

The TSL is purely phenomenological but certainly depends on the actual separation process. Its choice is up to the user and decides on the correct prediction of measured macroscopic data as load-displacement curves or crack-resistance curves. The effect of the various cohesive laws on the simulated crack extension has not been investigated systematically. Tvergaard & Hutchinson [19] studied the influence of the shape-parameters δ_1 and δ_2 in eq. (6) by varying them in the range of $\delta_1/\delta_c = 0.125 \div 0.15$ and $\delta_2/\delta_c = 0.25 \div 0.5$ and concluded that they have little effect on the steady state toughness of a material. Though this investigation covers only a small class of cohesive laws, it is often referenced as evidence that the shape of the cohesive law has little effect on the results. The crucial question is not whether a load-displacement curve for a specimen can be predicted with all

cohesive laws, but whether it is possible to transfer the material parameters from one cohesive law to another. Based on simulations with several of the functions introduced above, Scheider & Brocks [26] showed that the cohesive law significantly affects the results and once identified model parameters are bound to the chosen function, see also [5].

Mixed mode crack extension. All cohesive models can be used for normal and tangential separation as well as for combined loading. At combined normal and shear fracture the shear damage will reduce the ductility in normal direction and vice versa:

$$\sigma_\mathrm{n} = f_\mathrm{n}\left(\delta_\mathrm{n}, \delta_\mathrm{t}\right), \quad \sigma_\mathrm{t} = f_\mathrm{t}\left(\delta_\mathrm{n}, \delta_\mathrm{t}\right). \tag{9}$$

The interaction of shear and normal separation can be described by a damage variable, *D*, which is defined as

$$D = \left[\left(\frac{\langle\delta_\mathrm{n}\rangle}{\delta_\mathrm{n}^\mathrm{c}}\right)^\alpha + \left(\frac{\delta_\mathrm{t}}{\delta_\mathrm{t}^\mathrm{c}}\right)^\alpha\right]^{1/\alpha} \tag{10}$$

with an additional interaction parameter α [22], see Scheider (2000). Macauley brackets $\langle\square\rangle$ indicate that the effect of δ_n vanishes under compression. For $\alpha = 2$ and $\delta_\mathrm{n}^\mathrm{c} = \delta_\mathrm{t}^\mathrm{c} = \delta_\mathrm{c}$, the damage variable in eq. (10) equals to the normalized absolute value of separation, $\delta = \sqrt{\delta_\mathrm{n}^2 + \delta_\mathrm{t}^2}$, and $\alpha \to \infty$ defines a vanishing interaction of the separations.

Introducing *D*, the functions in eq. (87) can be written as

$$\sigma_\mathrm{n} = f_\mathrm{n}\left(\delta_\mathrm{n}, D\right), \quad \sigma_\mathrm{t} = f_\mathrm{t}\left(\delta_\mathrm{t}, D\right). \tag{11}$$

The cubic cohesive law, eq. (4), has been extended to combined normal and shear separation [13] with four independent cohesive parameters and $\alpha = 2$:

$$\sigma_\mathrm{n/t}(\delta) = \frac{27}{4}\sigma_\mathrm{n/t}^\mathrm{c}\,\frac{\delta_\mathrm{n/t}}{\delta_\mathrm{n/t}^\mathrm{c}}\left(1-D\right)^2. \tag{12}$$

A similar approach is used for the cohesive law proposed by Tvergaard & Hutchinson [20], eq. (6).

The exponential cohesive law, eq. (5), has been extended to mixed mode by Xu & Needleman [16]:

$$\left.\begin{aligned}
\sigma_\mathrm{n} &= \sigma_\mathrm{c}\, e \exp\left(-\frac{\delta_\mathrm{n}}{\delta_0}\right)\left[\frac{\delta_\mathrm{n}}{\delta_0}\exp\left(-\frac{\delta_\mathrm{t}}{\delta_0}\right)^2 + (1-q)\left[1-\exp\left(-\frac{\delta_\mathrm{t}}{\delta_0}\right)^2\right]\frac{\delta_\mathrm{n}}{\delta_0}\right] \\
\sigma_\mathrm{t} &= 2\sigma_\mathrm{c}\, e\, q\left(\frac{\delta_\mathrm{t}}{\delta_0}\right)\left(1+\frac{\delta_\mathrm{n}}{\delta_0}\right)\exp\left(-\frac{\delta_\mathrm{n}}{\delta_0}\right)\exp\left(-\frac{\delta_\mathrm{t}}{\delta_0}\right)^2
\end{aligned}\right\}, \tag{13}$$

where δ_0 is the separation at maximum normal traction, $\sigma_\mathrm{n}(\delta_0) = \sigma_\mathrm{c}$. It has only three model parameters, σc, δ_0, q ($0 \le q \le 1$). For $q = 1$, the separation energies of pure normal and pure shear fracture are equal and $q = 0.4289$ yields identical cohesive strengths for both fracture modes.

Unloading and reverse loading. Local unloading can occur in the cases of global unloading of a structure, crack branching or multiple cracks. Hence, assumptions on the behaviour of the cohesive elements under decreasing separation accounting for the irreversibility of the damage process have to be made. The terms “loading” and “unloading” will be used in the sense of increasing or decreasing separation, respectively. More generally, “unloading” is any change of the deformation by which the stress state deviates from the limiting traction-separation curve, which also applies for shear separation.

- In ductile materials**,** the mechanical work for producing damage is totally dissipated, the void growth and hence the inelastic separation are irreversible and any reduction of separation occurs purely elastically with unchanged elastic stiffness, see upper row of Fig. 3.
- In brittle materials, the elastic stiffness of the material is reduced by damage, but the separation vanishes when the stresses decrease to zero, see lower row of Fig. 3.

Negative normal separation is physically not admissible as it indicates penetration of the adjacent continuum elements. The stiffness of the cohesive element should hence be as high as possible, at least as high as the initial elastic stiffness. The contact condition, i.e. prevention of penetration of adjacent continuum elements, has to be ensured also after total failure of the cohesive element.

Unidirectional shear separation can be treated in the same way as normal separation. Reverse shear however requires a different model as damage may increase in both directions. In analogy to the isotropic hardening in the theory of plasticity, it is assumed that damage which has been activated by separation in one direction becomes also active in the opposite direction, if the same absolute value of shear stresses is reached. The shear stress will then follow the cohesive law again, whereas in between it varies linearly with the separation, see the right column in Fig. 3.

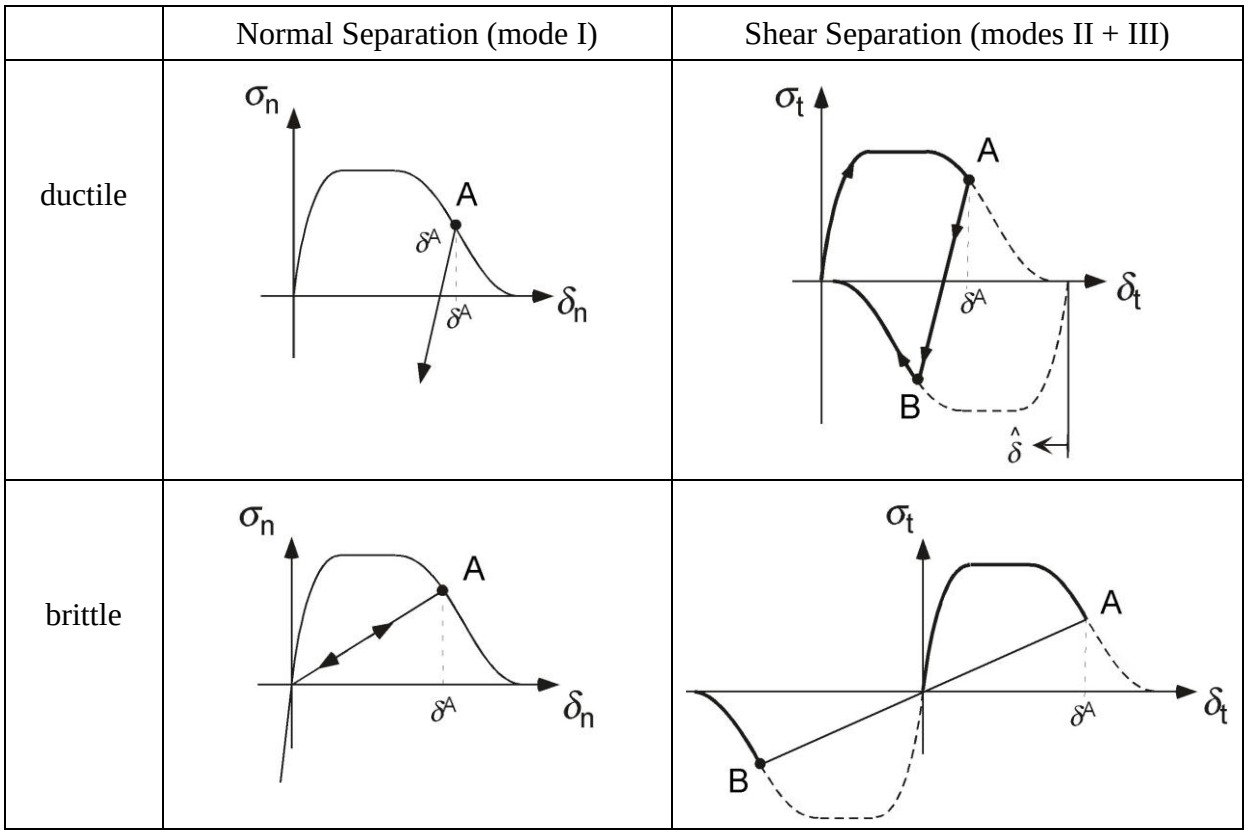

Fig. 3. Modelling of loading and reloading processes in the cohesive zone

Realisation in the framework of FEM. Common FE codes base on the principle of virtual work. The internal virtual work including cohesive elements writes

$$\delta \Pi_{\mathrm{i}} = \int_{\mathrm{B}} \mathbf{S} \cdot\cdot \delta \mathbf{E} \, \mathrm{d}V + \int_{\partial \mathrm{B}} \boldsymbol{\sigma} \cdot \delta \left[\mathbf{u} \right] \mathrm{d}S \,, \tag{14}$$

with **S** being the stress tensor, **E** the work conjugated strain tensor, and **σ** the vector of the tractions. For an incremental analysis the second term becomes

$$\delta\Delta\Pi_{\mathrm{i}} = \int_{\partial \mathrm{B}} \frac{\partial \boldsymbol{\sigma}}{\partial [\mathbf{u}]} \cdot \Delta[\mathbf{u}] \cdot \delta[\mathbf{u}] \, \mathrm{d}S$$
$$= \delta[\mathbf{u}] \cdot \left(\int_{\partial \mathrm{B}} \mathbf{V}_{\mathrm{u}}^{\mathrm{T}} \cdot \frac{\partial \boldsymbol{\sigma}}{\partial [\mathbf{u}]} \cdot \mathbf{V}_{\mathrm{u}} \, \mathrm{d}S \right) \cdot \Delta[\mathbf{u}]_{\mathrm{e}} = \delta[\mathbf{u}] \cdot \mathbf{K} \cdot \Delta[\mathbf{u}]_{\mathrm{e}} \quad ; \qquad (15)$$

where the field vector $\Delta[\mathbf{u}]$ is calculated by means of the matrix of shape functions $\mathbf{V}_{\mathrm{u}}$ and the separations at the nodes $[\mathbf{u}]_{\mathrm{e}}$, see Fig. 4a. The rank of $\mathbf{V}_{\mathrm{u}}$ depends on the degree of the shape functions describing the element geometry and displacements. $\mathbf{K}$ is the stiffness matrix of the cohesive element. The derivative of the tractions with respect to the separations can be calculated analytically from the given cohesive law. The integration over the surface of the cohesive element is done numerically in local coordinates and transformed into global ones afterwards. Adopting an updated Lagrangean formulation, the local coordinate system (ξ, η) is located in a mid section face bisecting the upper and lower surfaces and moves with the element, see Fig. 4b.

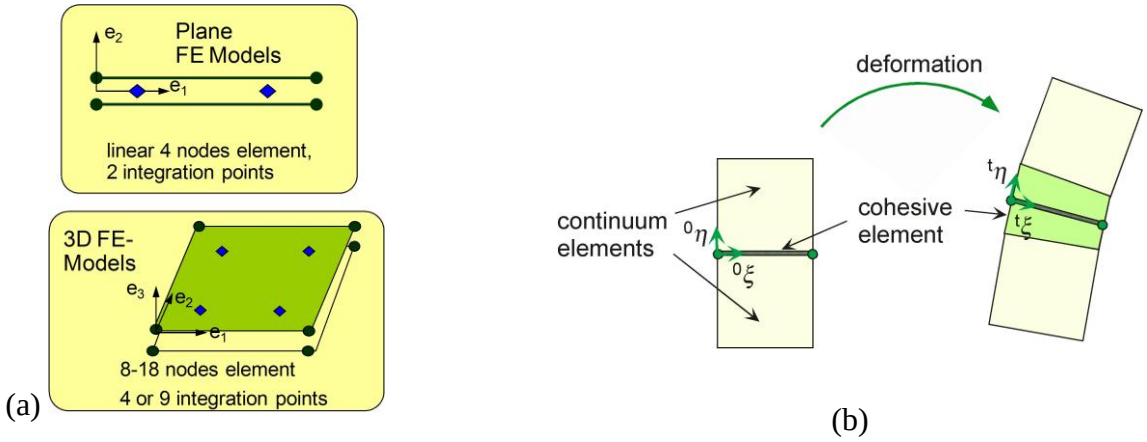

Fig. 4. Realisation of cohesive elements: (a) 2D and 3D FE models; (b) Local coordinate system.

Enhancements of the Cohesive Model

Effects of external variables on cohesive parameters. Up to now, the cohesive parameters have been regarded as material constants which do not depend on any other quantities. This is not mandatory, however. Several applications exist, where a dependence on external variables has been assumed like

- Changes of the thickness in analyses of thin-walled structures with plane stress or shell elements [27, 28],
- Triaxiality of the stress state for ductile damage processes [18],
- Strain rate for dynamic loading [29],
- Hydrogen concentration in a model of stress corrosion cracking [30],

and a dependence on temperature can be modelled likewise. Information on the actual values of these external parameters is obtained from the adjacent continuum elements and transferred to the cohesive elements, see Fig. 5a. In any case, this dependence has to be identified and described mathematically.

Numerical analyses of void growth in ductile materials [31-33] indicate that cohesive strength, σ_c, and separation energy, Γ_c, depend on the *triaxiality* of the stress state

$$T = \frac{\sigma_{\text{hyd}}}{\sigma_{\text{eq}}} = \frac{\frac{1}{3}\sigma_{kk}}{\sqrt{\frac{3}{2}\sigma'_{ij}\sigma'_{ij}}} . \tag{16}$$

The cohesive strength increases, the separation energy decreases with increasing triaxiality, see Fig. 5b, as is known from macroscopic tests.

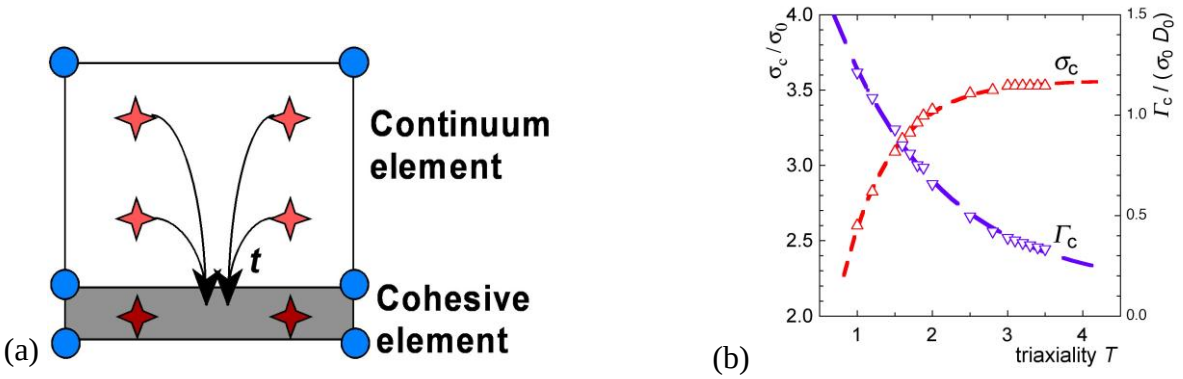

Fig. 5. Effect of external variables on cohesive parameters: (a) Transfer of information from continuum to cohesive elements; (b) Dependence of σ_c and Γ_c on stress triaxiality [33].

This dependence can be considered for the simulation of ductile crack extension [18]. Numerically predicted R-curves of fracture specimens under plane-strain conditions showed nearly no effect, however, as the separation energy contributes only negligibly to the globally dissipated work of plastic deformations [5, 34]. In addition, the dependence on the stress state is much less pronounced for higher triaxialities, see Fig. 5b.

Rate dependent cohesive laws. Rate and time dependent fracture phenomena require respective cohesive models. For most metals the rate effect is minor except for high temperatures or dynamic (impact) loading. These effects are of great interest for the fracture behaviour of polymers and the simulation of adhesives using the cohesive model, however. Therefore, most of the models described below are developed for the application to these materials.

A rate formulation of the TSL has the general form

$$\dot{\sigma} = f\left(\delta, \dot{\delta}, \sigma, \kappa_i\right), \tag{16}$$

where the variables κ_i are additional state variables (e.g. time, temperature, etc.).

The rate dependence can be introduced in different ways depending on the material behaviour:

(i) explicit rate dependence, (ii) viscoplastic behaviour, (iii) viscoelastic behaviour.

In the first case, the tractions depend explicitly on the separation rate,

$$\sigma = f\left(\delta, \dot{\delta}\right). \tag{17}$$

Some authors [35, 36] apply rheological models of the Kelvin-Voigt type, i.e. a (nonlinear) spring and a (nonlinear) dashpot in parallel, to describe this behaviour. The cohesive traction is the sum of the contributions of the spring and the dashpot,

$$\sigma = f_1(\delta) + f_2(\dot{\delta}). \tag{18}$$

A simplified form of this model assumes a frictional block instead of a spring and a linear dashpot.

$$\sigma(\delta,\dot{\delta}) = \sigma_0 + \eta\dot{\delta} \quad \text{for} \quad \delta < \delta_0 . \tag{19}$$

A model for crazing in homopolymers [37] contains the mixed term $(\dot{\delta}\cdot\delta)$ and thus cannot be represented by a spring-dashpot combination according to eq. (16). It is based on the linear decreasing law, Fig. 2a, with an embedded rate dependency:

$$\sigma(\delta,\dot{\delta}) = \left(\sigma_0 + \eta\dot{\delta}\right)\left(1-\frac{\delta}{\delta_0}\right). \tag{20}$$

In *viscoplastic* cohesive laws, the separation is split in an elastic and a viscoplastic part as in respective constitutive relations of continuum mechanics,

$$\delta = \delta^{\mathrm{el}} + \delta^{\mathrm{vp}}, \tag{21}$$

where the elastic part is defined by any of the cohesive laws described above,

$$\sigma = f\left(\delta - \delta^{\mathrm{vp}}\right). \tag{22}$$

and δ^{vp}, is given by some viscoplastic law, for instance [38]

$$\dot{\delta}^{\mathrm{vp}} = \dot{\delta}_0 \exp\left[\frac{-A^{\mathrm{c}}\sigma^{\mathrm{c}}}{\theta}\left(1-\frac{\sigma}{\sigma_0}\right)\right], \tag{23}$$

depending on the temperature, θ, with A^{c}, σ^{c}, and $\dot{\delta}_0$ being model parameters.

Corigliano & Ricci [39] proposed a viscoplastic law for the separation vector $\boldsymbol{\delta}^{\mathrm{vp}} = \left\{\delta_{\mathrm{n}}^{\mathrm{vp}}, \delta_{\mathrm{t}}^{\mathrm{vp}}\right\}$,

$$\begin{aligned}
\dot{\delta}_{\mathrm{n}}^{\mathrm{vp}} &= \left\langle f(\sigma_{\mathrm{n}},\sigma_{\mathrm{t}},\delta_{\mathrm{acc}}^{\mathrm{vp}})\right\rangle^{n} \frac{\partial f(\sigma_{\mathrm{n}},\sigma_{\mathrm{t}},\delta_{\mathrm{acc}}^{\mathrm{vp}})}{\partial\sigma_{\mathrm{n}}} \\
\dot{\delta}_{\mathrm{t}}^{\mathrm{vp}} &= \left\langle f(\sigma_{\mathrm{n}},\sigma_{\mathrm{t}},\delta_{\mathrm{acc}}^{\mathrm{vp}})\right\rangle^{n} \frac{\partial f(\sigma_{\mathrm{n}},\sigma_{\mathrm{t}},\delta_{\mathrm{acc}}^{\mathrm{vp}})}{\partial\sigma_{\mathrm{t}}}
\end{aligned}, \tag{24}$$

with

$$f(\sigma_{\mathrm{n}},\sigma_{\mathrm{t}},\delta_{\mathrm{acc}}^{\mathrm{vp}}) = \sqrt{a_{\mathrm{n}}\left\langle\sigma_{\mathrm{n}}\right\rangle^2 + a_{\mathrm{t}}\sigma_{\mathrm{t}}^2} - 1 + h\,\delta_{\mathrm{acc}}^{\mathrm{vp}}. \tag{25}$$

The accumulated viscoplastic separation, $\delta_{\mathrm{acc}}^{\mathrm{vp}}$, is defined as

$$\delta_{\mathrm{acc}}^{\mathrm{vp}} = \int_0^t \sqrt{\left(\dot{\delta}_{\mathrm{n}}^{\mathrm{vp}}\right)^2 + \left(\dot{\delta}_{\mathrm{t}}^{\mathrm{vp}}\right)^2}\,\mathrm{d}\tau\,, \tag{26}$$

and a_{n}, a_{t}, n and h are model parameters.

Viscoelastic cohesive laws are of increasing interest mainly for elastomers and fiber/matrix composites. The nonlinear Kelvin-Voigt model of eq. (16) describes viscoelastic behavior. Alternatively, a functional formulation can be chosen where the time-dependent tractions, $\sigma(\delta,t)$, result from a time integral over the separation history, multiplied by some time-independent function, $\sigma_{\mathrm{stat}}(\delta)$, which can be any of the cohesive laws shown in Fig.2, [40],

$$\sigma(\delta,t) = \sigma_{\mathrm{stat}}(\delta)\int_0^t G(t-\tau)\,\dot{D}\,\mathrm{d}\tau\,, \tag{27}$$

or from a damage law with an additional threshold value σ_0 [41],

$$\sigma(\delta,t)=\left[1-\alpha(t)\right]\left[\sigma_0+\int_0^t E^{\mathrm{ve}}(t-\tau)\dot{D}\,\mathrm{d}\tau\right]. \tag{28}$$

A rather simple standard viscoelastic linear model is used for the relaxation module $E_{ve}(t - t')$, which writes

$$E^{\mathrm{ve}}(t-t')=E_{\infty}^{\mathrm{ve}}+E_0^{\mathrm{ve}}\exp(-t/t'). \tag{29}$$

Fatigue crack growth. Current predictions of fatigue life are based on phenomenological laws, relating the amplitude of the applied stress intensity factor, ΔK, to the crack growth rate, da/dN, like the well known Paris law, which describes the fatigue crack growth under small scale yielding conditions and constant amplitude loading. A further restriction is its applicability to long cracks only. Cohesive modelling can provide an alternative approach, which is in general not restricted to size and geometry requirements, crack lengths or loading conditions. Note, however, that linear un- and reloading described in Fig. 3 is not capable to model crack growth under cyclic loading, but predict shake down and crack arrest in a structure [42].

Cohesive laws with an *unloading-reloading hysteresis* as shown in Fig. 6 have been introduced by Yang et al. [43] and Nguyen et al. [44]. Linear unloading combined with nonlinear reloading allowed for phenomenological descriptions of dissipative mechanisms such as frictional interactions between asperities as well as crystallographic slip.

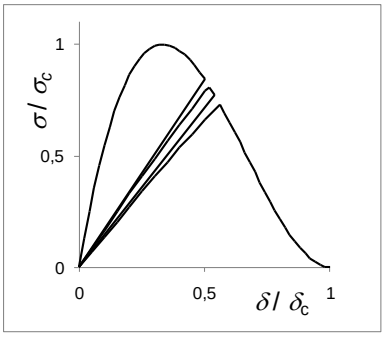

Fig. 6. Hysteresis behaviour during loading and reloading processes for simulation of cyclic softening

Roe and Siegmund [45] proposed a model, in which the traction-separation behaviour of a cohesive element follows the cohesive law of eq. (5), but cyclic damage evolution decreases the cohesive strength,

$$\sigma_{\mathrm{c}}^{\mathrm{fat}}=\sigma_{\mathrm{c}}\left(1-D_{\mathrm{acc}}\right), \tag{30}$$

where D_{acc} is the accumulated damage accounting for the separation history. It is calculated by an evolution law including a threshold value. Different from [43, 44], Fig. 6, the unloading and reloading paths were assumed to be identical.

These models [43-45] require a simulation of every load cycle and are hence restricted to a rather low number of cycles. DeAndrés et al. [46] calculated the evolution of damage in a cohesive element for a few loading cycles and then extrapolated to a larger number of cycles by

$$D_{n+1}=D_n+\left.\frac{\partial D}{\partial N}\right|_n\left(N_{n+1}-N_n\right). \tag{31}$$

They applied an exponential cohesive law with a linear unloading-reloading option to predict crack extension in a surface-notched round bar under high cycle fatigue loading. By repeated extrapolation and determination of the damage rate $\partial D/\partial N$ more than 300.000 cycles were simulated.

Fig 6 points to an additional problem with respect to the applied TSL. Cyclic softening due to an unloading-reloading hysteresis occurs after maximum stress, and the value of the latter obviously

has to differ from the cohesive strength for monotonic loading. Hence, the cyclic TSL has to be different from the static one. The same holds for eq. (31), basically, but since σ_c^{fat} decreases with accumulated damage, the evolution law for D_{acc} will affect the appropriate choice of σ_c.
Considering the various open problems, modelling of fatigue crack growth by a cohesive approach is far less understood and established than modelling of crack extension under monotonous loading.

Parameter Identification

Cohesive laws and cohesive parameters cannot be measured directly. Their identification is, as for many nonlinear problems, an *inverse process* of minimising the differences between measured and simulated macroscopic test data [47]. Uniqueness of parameters is a key issue as the idea is to transfer values, which have been determined from test specimens to analyses of other configurations [26], particularly large scale structures. Studies on parameter identification are reported in [11, 48, 49].

Summary

The cohesive model can be regarded as a flexible, versatile and robust tool for computational simulations of damage localisation and material separation up to structural failure. Due to its phenomenological character, the model is adjustable to many different types of materials and failure phenomena. Cohesive laws can be established for various separation phenomena and can also be extended to time-dependent material behaviour. Separation processes, damage and fracture on *different length scales* can be simulated. The model can be applied to analyses of macroscopic engineering structures as well as heterogeneous microstructures. The restriction to crack paths which are predefined by the FE mesh can be a drawback in cases where nothing is known about possible directions of crack propagation. Crack branching has been simulated successfully, nevertheless [24, 50].

Within certain limits, the cohesive relation can be regarded as a material law, and the respective parameters characterise material properties with respect to damage and fracture independent of a specific geometry. There are no problems as in classical macroscopic fracture mechanics with transferring the parameters from small specimens to large components.

Cohesive models endow materials with a *characteristic length*, and unlike damage theories, a cohesive law introduces a well-defined fracture energy, which eliminates mesh dependence, so that finite element solutions attain proper convergence in the limit of vanishing mesh size.

References

[1] G.I. Barenblatt: Appl. Math. Mech. Vol. 23 (1959), p. 623.
[2] G.I. Barenblatt: Adv. Appl. Mech. Vol. 7 (1962), p. 55.
[3] A. Hillerborg, M. Modeer and P,E. Petersson: Cement Concrete Res. Vol. 6 (1976), p. 773.
[4] W. Brocks: Struct. Integr. Durab. Vol. 1 (2005), p. 233.
[5] W. Brocks, A. Cornec and I. Scheider, in: *Comprehensive Structural Integrity*, edited by I. Milne, R.O. Ritchie and B. Karihaloo, Vol. 3, Elsevier (2003), p. 127.
[6] K.-H. Schwalbe, I. Scheider and A. Cornec: *The SIAM method for applying cohesive models to the damage behaviour of engineering materials and structures*. Report GKSS 2009/1, Helmholtz Centre Geesthacht, Germany, 2009.
[7] Th. Siegmund and W. Brocks: Int. J. Fract. Vol. 99 (1999), p. 97.
[8] H. Krull and H. Yuan, H: Eng. Fract. Mech. Vol. 78 (2011), p. 525.
[9] Z.P. Bažant, in: *Proc. 5th Int. RILEM Symp. on Creep and Shrinkage of Concrete*, edited by Z.P. Bažant and I. Carol, E & FN Spon (1993), London and New York, p. 291.

[10] Z.P. Bažant: Eng. Fract. Mech. Vol. 69 (2003), p. 165.
[11] G. Maier, M. Bocciarelli, G. Bolzon and R. Fedele: Int. J. Fracture Vol. 138 (2006), p. 47.
[12] A. Needleman: J. Appl: Mech. Vol. 54 (1987), p. 525.
[13] V. Tvergaard: Mater. Sci. Eng. A Vol. 190 (1990), p. 203.
[14] A. Needleman: Int. J. Fracture Vol. 42 (1990), p. 21.
[15] J. Rose, J. Ferrante and J. Smith: Phys. Rev. Lett. Vol. 75 (1981), p. 675.
[16] X. Xu and A. Needleman: J. Mech. Phys. Solids Vol. 42 (1994), p. 1397.
[17] T. Siegmund and A. Needleman: Int. J. Solids Struct. Vol. 34 (1997), p. 769.
[18] T. Siegmund and W. Brocks: Engng. Fract. Mech., Vol. 67 (2000), p. 139.
[19] V. Tvergaard and J.W. Hutchinson: J. Mech. Phys. Solids Vol. 40 (1992), p. 1377.
[20] V. Tvergaard and J.W. Hutchinson: J. Mech. Phys. Solids Vol. 41 (1993), p. 1119.
[21] G. Lin, A. Cornec and K.H. Schwalbe: Fatigue Fract. Eng. Mater. Struct. Vol. 21 (1998), p. 1159.
[22] I. Scheider: *PhD Thesis*, TU Hamburg-Harburg, Report GKSS 2001/3, Helmholtz Centre Geesthacht, Germany, 2001.
[23] I. Scheider: Eng. Fract. Mech. Vol. 76 (2009), p. 1450.
[24] I. Scheider and W. Brocks: Eng. Fract. Mech. Vol. 70 (2003), p. 1943.
[25] M. Elices, G.V. Guinea, J. Gómez and J. Planas: Eng. Fract. Mech. Vol. 69 (2002), p. 137.
[26] I. Scheider and W. Brocks: Key Engng. Mater. Vols. 251-252 (2003), p. 313.
[27] I. Scheider and W. Brocks: Comp. Mater. Sci. Vol. 37 (2003), p. 101.
[28] I. Scheider, M. Schödel, W. Brocks and W. Schönfeld: Eng. Fract. Mech. 73 (2006), p. 252.
[29] M. Anvari, C. Thaulow and I. Scheider: Eng. Fract. Mech. Vol. 73 (2006), p. 2210.
[30] R. Falkenberg, W. Brocks, W. Dietzel, and I. Scheider: Int. J. Mat. Res. Vol. 101 (2010), p. 989.
[31] J. Koplik and A. Needleman: Int. J. Solids Struct. Vol. 24 (1988), p. 835.
[32] W. Brocks, D.-Z. Sun and A. Hönig: Int. J. Plasticity Vol. 11 (1995), p. 971.
[33] T. Siegmund and W. Brocks, W.: Int. J. Fracture , Vol. 99 (1999), p. 97.
[34] W. Brocks, P. Anuschewski and I. Scheider: Engng. Fail. Anal. Vol. 17 (2010), p. 607.
[35] K.M. Liechti and J.D. Wu: J. Mech. Phys. Solids Vol. 49 (2001), p.1039.
[36] F. Costanzo and J.R. Walton: Int. J. Eng. Sci. Vol. 35 (1997), p. 1085.
[37] D.B. Xu, C.Y. Hui, E.J. Kramer and C. Creton: Mech. Mater. Vol. 11 (1991), p. 257.
[38] R. Estevez, M.G.A. Tijssens and E. van der Giessen: J. Mech. Phys. Solids, Vol. 48 (2000), p. 2585.
[39] A. Corigliano and M. Ricci: Int. J Solids Struct. Vol. 38 (2001), p. 547.
[40] P. Rahul-Kumar, A. Jagota, S.J. Bennison, S. Saigal and S. Muralidhar: Acta Mater. Vol. 47 (1999), p. 4161.
[41] D.H. Allen and C.R. Searcy: Int. J. Fract. Vol. 107 (2001), p. 159.
[42] B. Yang and K. Ravi-Chandar: Int. J. Fract. Vol. 93 (1998), p. 115.
[43] B. Yang, S. Mall and K. Ravi-Chandar: Int. J. Solids. Struct. Vol. 38 (2001), p.3927.
[44] O. Nguyen, E.A. Repetto, M. Ortiz and R.A. Radovitzki: Int. J. Fracture Vol. 110 (2001), p. 351.
[45] K.L. Roe and T. Siegmund: Eng. Fract. Mech. Vol. 70 (2003), p. 209.
[46] A. de Andrés, J.L. Perez and M. Ortiz: Int. J. Solids Struct. Vol. 36 (1999), p. 2231.
[47] W. Brocks and D. Steglich in: *Comprehensive Structural Integrity* edited by I. Milne, R.O. Ritchie and B. Karihaloo, Online Update Vol. 11 (2007), Elsevier, p. 107.
[48] G. Bolzon, G. Maier and M. Panico: Int. J. Solids Struct. Vol. 41 (2004), p. 2957.
[49] W. Brocks and I. Scheider: Struct. Durab. Health Monit. Vol. 161 (2010), p. 1-24.
[50] W. Brocks and I. Scheider: Struct. Durab. Health Monit. Vol. 70 (2008), p. 1.